Electronic Supplementary Material (ESI) for ChemComm.

Chiral cyclic architectonics with tetraphenylethylenes: conformation immobilization, optical resolution and circularly polarized luminescence

Qi Meng, Liwen Cui, Qi Liao, Jian Xu* and Yuxiang Wang*

Jiangsu Province Key Laboratory of Fine Petrochemical Engineering, School of Petrochemical Engineering, Changzhou University, Changzhou 213164, China. E-mail: wangyx@cczu.edu.cn

Table of Contents

1. Measurements and Materials

Nuclear magnetic resonance (NMR) spectra were recorded on 300 MHz Bruker spectrometer with TMS as the internal standard. Ultraviolet-visible (UV-*vis*) spectra were recorded on Shimadzu UV-1700 UV-*vis* spectrophotometer. Emission spectra were performed on Agilent Cary Eclipse spectrophotometer. The transient photoluminescence (PL) decay spectra and absolute PL quantum yield were determined by Edinburgh FS5 Fluorescence Spectrometer. Circular dichroism (CD) spectra were measured from a JASCO J-810 spectropolarimeter. CPL spectra were measured from a JASCO CPL-300 spectrofluoropolarimeter. The enantiomeric excesses were confirmed by chiral HPLC using an Agilent 1200 LC instrument with a Daicel CHIRALPAK® AD and OD column (solvent flow rate 1.0 L/min).

The single crystals of **(*R*)-*p*TPE** and **(*R*)-*o*TPE1** were obtained by volatilizing the solution of CH_2Cl_2/CH_3OH at room temperature, the single crystals of ***rac*-*o*TPE2** and **(*S*)-*o*TPE3** were obtained by volatilizing the solution of *i*-PrOH at room temperature. X-ray data at 150 K and 170 K were examined on a Bruker SMART APEX II Single-Crystal X-Ray Diffractometer using MoKα radiation (λ = 0.71073 Å). The structures were solved by direct methods and refined with the full-matrix least square technique. The details of crystal data and structure refinement were presented in Table S6. The crystal data of **(*R*)-*p*TPE**, **(*R*)-*o*TPE1, *rac*-*o*TPE2** and **(*S*)-*o*TPE3** were deposited to CCDC with CCDC number of 2182870, 2182873, 2182878 and 2182879.

2. Synthesis procedures of the chiral cyclic TPEs

Synthesis of (*R*)-*p*TPE. Compound **1** (100.00 mg, 0.19 mmol) and (*R*)-BINOL (55.24 mg, 0.19 mmol) were dissolved in anhydrous dimethylformamide (DMF, 10 mL), which was slowly added dropwise to anhydrous DMF solution (20 mL) containing anhydrous potassium carbonate (106.66 mg, 0.77 mmol) under N_2 atmosphere at 80 ℃. After stirring for 12 h, the mixture was cooled to room temperature, the reaction mixture was washed with water and extracted with ethyl acetate. The organic phase was dried with anhydrous Na_2SO_4 and the solvent was evaporated. The reaction mixture was purified by column chromatography (petroleum ether/ethyl acetate = 80:1) to afford the **(*R*)-*p*TPE** (35.20 mg, 28%) as a white powder. ^{1}H NMR (300 MHz, $CDCl_3$): δ 7.97 (d, J = 9.0 Hz, 2H), 7.88 (d, J = 8.0 Hz, 2H), 7.58 (d, J = 9.1 Hz, 2H), 7.33 (t, J = 6.8 Hz, 2H), 7.22 (d, J = 6.7 Hz, 2H), 7.16 (d, J = 8.2 Hz, 12H), 6.63 (s, 8H), 5.04 (d, J = 11.8 Hz, 2H), 4.75 (d, J = 11.8 Hz, 2H). ^{13}C NMR (75 MHz, $CDCl_3$): δ 153.87, 144.18, 141.92, 141.68, 135.39, 134.72, 131.19, 129.28,

128.95, 128.18, 127.95, 126.95, 126.35, 125.73, 123.66, 120.82, 116.12, 70.36. HRMS (ESI, m/z): caled for $C_{48}H_{35}O_2$ [M + H^+], 643.2632; found, 643.2634.

Synthesis of (*S*)-*p*TPE. Compound **1** (200.00 mg, 0.31 mmol) and (*S*)-BINOL (110.49 mg, 0.39 mmol) were dissolved in anhydrous dimethylformamide (DMF, 10 mL), which was slowly added dropwise into 25 mL anhydrous DMF solution containing anhydrous potassium carbonate (213.32 mg, 1.54 mmol) under N_2 atmosphere at 80 ℃. After stirring for 12 h, the mixture was cooled to room temperature, the reaction mixture was washed with water and extracted with ethyl acetate. The organic phase was dried with anhydrous Na_2SO_4 and the solvent was evaporated. The reaction mixture was purified by column chromatography (petroleum ether/ethyl acetate = 80:1) to afford **(*S*)-*p*TPE** (65.00 mg, 26%) as a white powder.

Synthesis of 2. In a two-necked round bottom flask were placed 1,1-Di(2-methylphenyl)-2,2--diphenylethylene (1.40 g, 4.13 mmol), N-bromosuccinimide (1.59 g, 8.93 mmol) and a catalytic amount of benzoyl peroxide, then 35 mL of carbon tetrachloride was added. The mixture was refluxed for 5 h. After cooling to room temperature, the reaction mixture was poured into 80 mL water and extracted with ethyl acetate. The organic layer was dried over anhydrous Na_2SO_4 and the solvent was evaporated. Then the residue was purified by column chromatography (petroleum ether) to afford product **2** (1.29 g, 64%) as a pale-yellow oil. ^{1}H NMR (300 MHz, $CDCl_3$): δ 7.37-7.30 (m, 2H), 7.22-7.06 (m, 16H), 4.45 (dd, J_1 = 10.4 Hz, J_2 = 10.4 Hz, 2H), 4.14 (dd, J_1 = 10.4 Hz, J_2 = 10.4 Hz, 2H). ^{13}C NMR (75 MHz, $CDCl_3$): δ 142.47, 142.11, 141.93, 140.31, 140.25, 136.42, 135.74, 132.91, 132.59, 131.81, 131.44, 131.26, 131.00, 130.58, 130.43, 128.62, 128.33, 128.23, 128.14, 128.09, 128.03, 127.89, 127.14, 127.04, 32.48, 32.24.

Synthesis of (*R*)-*o*TPE1 to **(*R*)-*o*TPE3.** Under N_2 atmosphere at 80 ℃, 16 mL anhydrous DMF solution containing compound **2** (600.00 mg, 1.16 mmol) was slowly added dropwise into 40 mL anhydrous DMF solution containing (*R*)-BINOL (331.47 mg, 1.16 mmol) and anhydrous potassium carbonate (639.97 mg, 4.63 mmol). After stirring overnight, the mixture was cooled to room temperature. Then the reaction mixture was washed with water and extracted with ethyl acetate. The organic phase was dried with anhydrous Na_2SO_4 and solvent was evaporated. The reaction mixture was purified by column chromatography (petroleum ether/ethyl acetate = 100:1) to afford three products all as a white powder.

(*R*)-*o*TPE1 (74.80 mg, 10%). ^{1}H NMR (300 MHz, $CDCl_3$): δ 7.81 (d, J = 8.0 Hz, 2H), 7.73 (d, J =

9.1 Hz, 2H), 7.28-7.23 (m, 4H), 7.13-7.10 (m, 2H), 7.07 (d, J = 1.1 Hz, 2H), 7.04 (d, J = 4.3 Hz, 1H), 7.02 (t, J = 2.4 Hz, 1H), 7.00 (t, J = 1.4 Hz, 1H), 6.98-6.95 (m, 4H), 6.78 (d, J = 8.6 Hz, 6H), 6.71 (t, J = 10.0 Hz, 5H), 4.58(d, J = 10.3 Hz, 2H), 4.32(d, J = 10.2 Hz, 2H). ^{13}C NMR (75 MHz, $CDCl_3$): δ 154.51, 142.67, 140.73, 140.24, 135.73, 134.77, 133.70, 131.20, 130.47, 128.91, 128.40, 127.80, 127.72, 127.60, 126.58, 126.14, 126.00, 125.49, 123.03, 118.46, 113.84, 69.20. HRMS (ESI, m/z): caled for $C_{48}H_{34}O_2Na$ [M + Na^+], 665.2451; found, 665.2454.

(*R*)-*o*TPE2 (59.70 mg, 8%). ^{1}H NMR (300 MHz, $CDCl_3$): δ 7.92 (d, J = 9.1 Hz, 2H), 7.87 (d, J = 8.1 Hz, 2H), 7.53 (d, J = 9.1 Hz, 2H), 7.45 (d, J = 7.5 Hz, 2H), 7.30 (d, J = 6.7 Hz, 2H), 7.23-7.16 (m, 3H), 7.12 (d, J = 9.1 Hz, 2H), 7.08-6.95 (m, 5H), 6.80 (t, J = 7.3 Hz, 2H), 6.61 (t, J = 7.3 Hz, 4H), 6.47 (d, J = 7.4 Hz, 4H), 4.69 (d, J = 14.2 Hz, 2H), 4.20 (d, J = 14.1 Hz, 2H). ^{13}C NMR (75 MHz, $CDCl_3$): δ 155.05, 142.48, 140.63, 140.47, 138.22, 134.34, 134.01, 131.14, 129.36, 128.98, 128.80, 127.85, 127.43, 126.84, 126.21, 125.94, 125.30, 123.26, 119.76, 115.18, 70.53. HRMS (ESI, m/z): caled for $C_{48}H_{34}O_2K$ [M + K^+], 681.2190; found, 681.2182.

(*R*)-*o*TPE3 (55.00 mg, 7%). ^{1}H NMR (300 MHz, $CDCl_3$): δ 7.84 (q, J = 8.6 Hz, 4H), 7.61 (d, J = 7.3 Hz, 1H), 7.49 (d, J = 9.1 Hz, 1H), 7.37-7.30 (m, 3H), 7.24 (d, J = 6.9 Hz, 1H), 7.19 (q, J = 1.7 Hz, 1H), 7.17-7.15 (m, 2H), 7.12-7.07 (m, 7H), 7.03-7.00 (m, 2H), 6.99-6.89 (m, 3H), 6.79 (d, J = 7.5 Hz, 1 H), 6.70 (t, J = 7.9 Hz, 2H), 6.46 (d, J = 7.1 Hz, 2H), 5.17 (d, J = 10.7 Hz, 1H), 4.73 (d, J = 14.5 Hz, 1H), 4.25 (d, J = 14.5 Hz, 1H), 3.93 (d, J = 10.7 Hz, 1H). ^{13}C NMR (75 MHz, $CDCl_3$): δ 156.35, 154.69, 143.57, 143.39, 142.10, 141.10, 140.34, 139.89, 136.07, 135.27, 134.60, 134.37, 134.24, 132.89, 132.08, 131.18, 130.88, 129.81, 129.59, 129.38, 129.15, 127.95, 127.89, 127.73, 127.59, 127.34, 127.11, 127.06, 126.73, 126.63, 126.45, 125.36, 125.30, 124.17, 123.97, 122.53, 120.45, 119.40, 117.59, 72.00, 69.92. HRMS (ESI, m/z): caled for $C_{48}H_{34}O_2Na$ [M + Na^+], 665.2451; found, 665.2441.

Synthesis of (*S*)-*o*TPE. Under N_2 atmosphere at 80 °C, 40 mL anhydrous DMF solution containing compound **2** (1.00 g, 1.93 mmol) was slowly added dropwise into 100 mL anhydrous DMF solution containing (*S*)-BINOL (552.45 mg, 1.93 mmol) and anhydrous potassium carbonate (1.07 mg, 7.74 mmol). After stirring overnight, the mixture was cooled to room temperature. Then the reaction mixture was washed with water and extracted with ethyl acetate. The organic phase was dried with anhydrous Na_2SO_4 and solvent was evaporated. The reaction mixture was purified by column chromatography (petroleum ether/ethyl acetate = 100:1) to afford three products all as a white

powder. **(*S*)-*o*TPE1** (179.00 mg, 14%), **(*S*)-*o*TPE2** (98.00 mg, 8%) and **(*S*)-*o*TPE3** (51.00 mg, 4%).

3. Photophysical Properties of the chiral cyclic TPEs

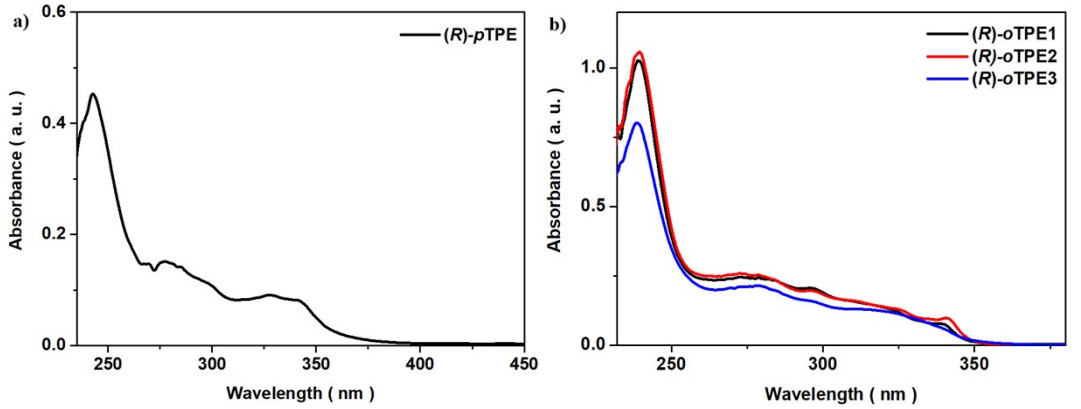

Figure S1. UV spectra of **(*R*)-*p*TPE** and **(*R*)-*o*TPE1** to **(*R*)-*o*TPE3** in THF solution (*ca*. 10^{-5} M).

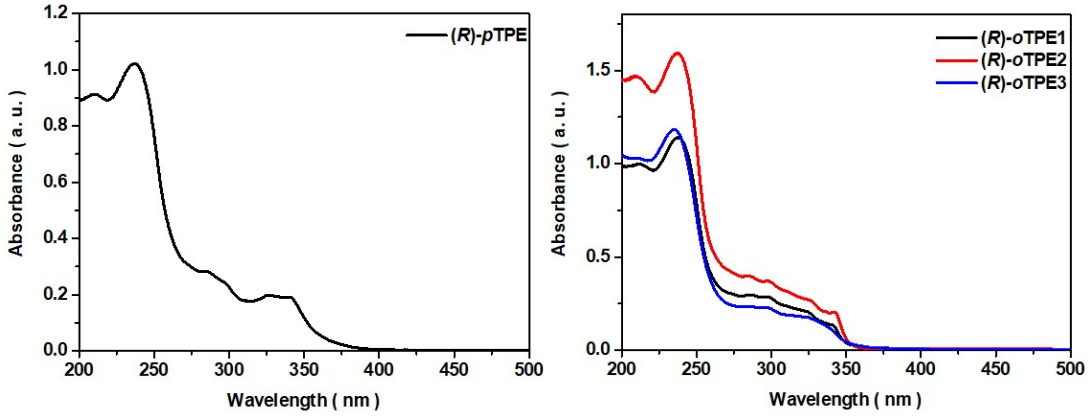

Figure S2. UV spectra of **(*R*)-*p*TPE** and **(*R*)-*o*TPE1** to **(*R*)-*o*TPE3** in the film state.

Table S1. Photophysical properties of the chiral cyclic TPEs.

Compound	THF solution				Film			
	λ_{abs} (nm)	λ_{em} (nm)	τ (ns)	Φ_F (%)	λ_{abs} (nm)	λ_{em} (nm)	τ (ns)	Φ_F (%)
(*R*)-*p*TPE	242, 278 340	497	1.96	1.5	238, 285 340	476	5.31	32.6
(*R*)-*o*TPE1	239, 273 339	417	3.89	22.4	238, 287 340	414	1.49	23.4
(*R*)-*o*TPE2	239, 273 341	405	4.38	15.5	237, 287 342	402	1.44	33.4
(*R*)-*o*TPE3	239, 278 312	405	4.50	0.2	235, 294 324	452	3.68	21.0

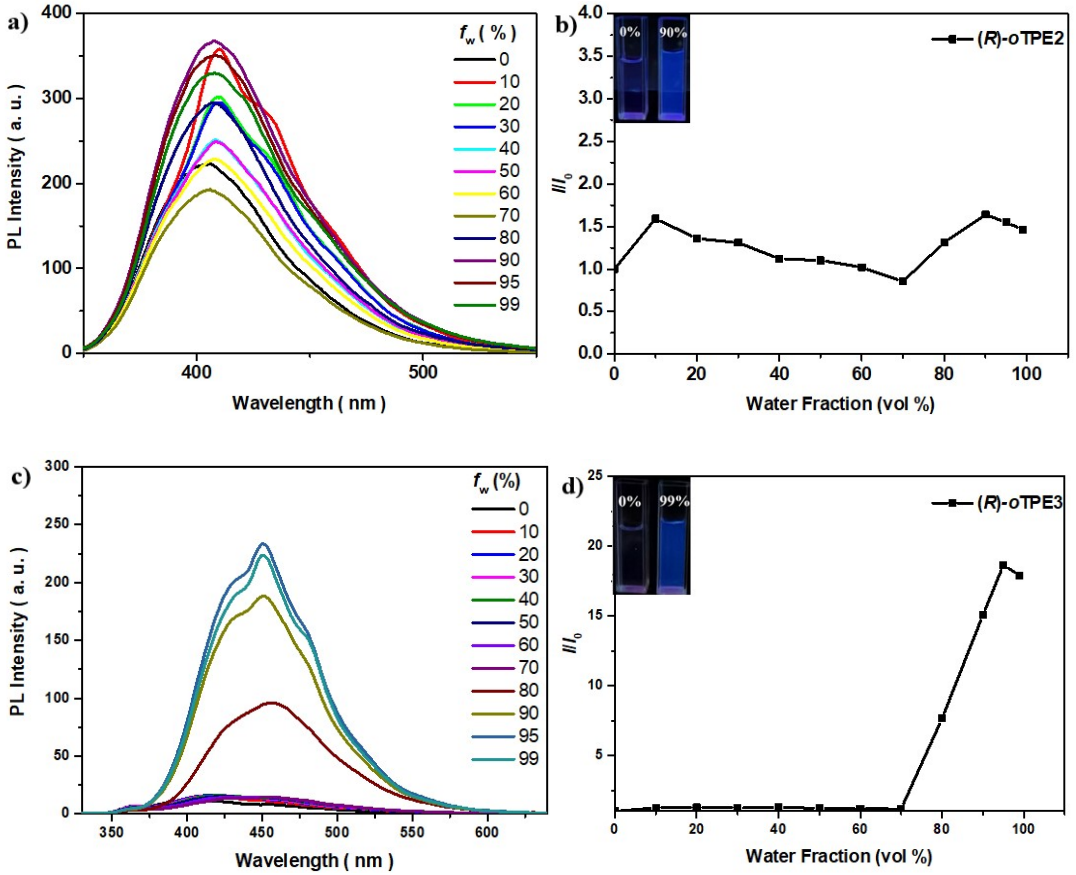

Figure S3. (a, c) Fluorescence spectra of **(*R*)-*o*TPE2** and **(*R*)-*o*TPE3** in H_2O/THF mixtures with different water fraction (f_w / %). (b, d) the relative fluorescence intensity to f_w, inset: photographs taken under UV illumination (365 nm).

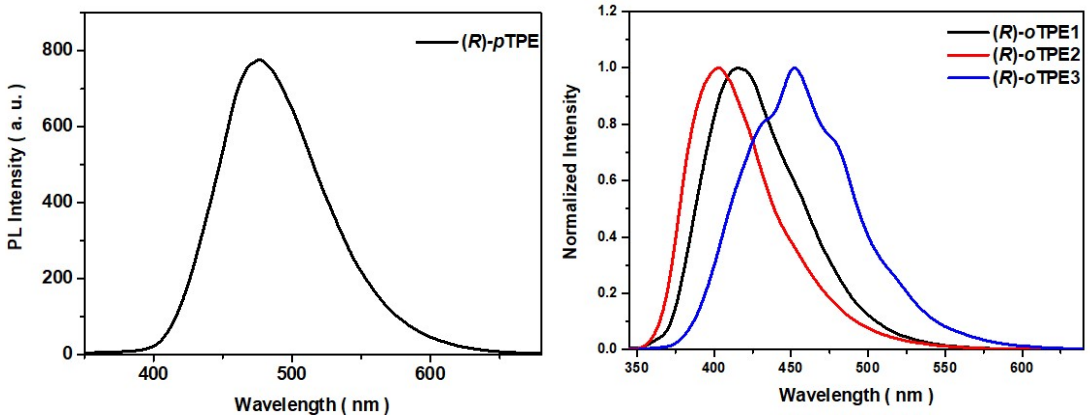

Figure S4. Fluorescence spectra of **(*R*)-*p*TPE** and **(*R*)-*o*TPE1** to **(*R*)-*o*TPE3** in the film state.

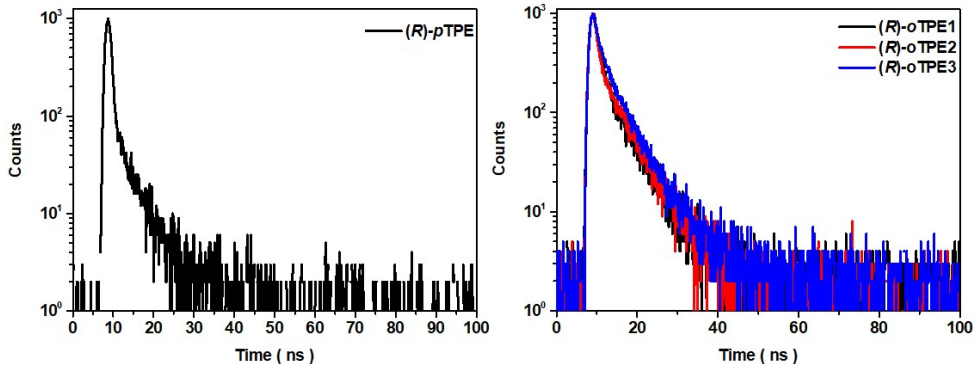

Figure S5. Transient PL decay spectra of **(*R*)-*p*TPE** and **(*R*)-*o*TPE1** to **(*R*)-*o*TPE3** in THF solution (*ca*. 10^{-5} M).

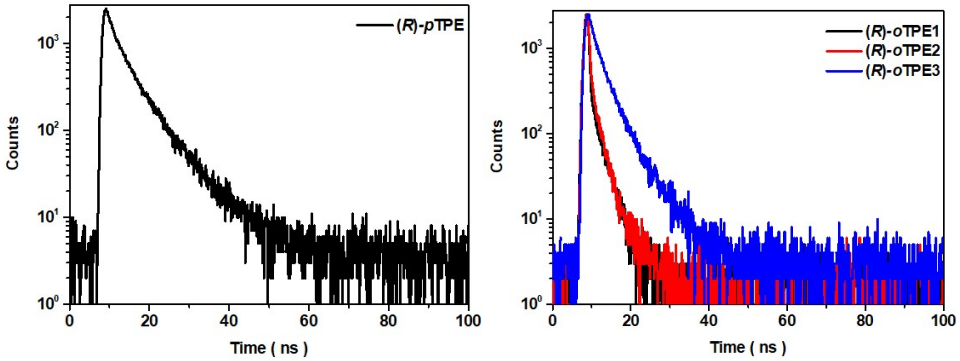

Figure S6. Transient PL decay spectra of **(*R*)-*p*TPE** and **(*R*)-*o*TPE1** to **(*R*)-*o*TPE3** in the film state.

Table S2. Transient PL decay data of the chiral cyclic TPEs in THF solutions and films.[a]

Compound	State	<τ> [ns]	τ_1 [ns]	τ_2 [ns]	A_1	A_2
(*R*)-*p*TPE	THF solution	2.0	0.6	4.7	1166.4	75.9
	film	5.3	2.3	6.8	1476.2	979.2
(*R*)-*o*TPE1	THF solution	3.9	1.3	5.7	790.8	265.3
	film	1.5	0.3	2.7	2477.9	279.7
(*R*)-*o*TPE2	THF solution	4.4	1.0	5.8	772.7	3113.8
	film	1.4	0.4	2.4	2155.3	425.6
(*R*)-*o*TPE3	THF solution	4.5	1.5	5.7	642.3	438.1
	film	3.7	1.8	4.8	1498.5	909.7

[a]Fluorescence lifetimes data were fitted by multiple-exponential function and the mean fluorescence

lifetimes (<τ>) were calculated by = $\Sigma A_i\tau_i^{\ 2} / \Sigma A_i\tau_i$, where A_i is the preexponential factors for τ_i.

4. Chiroptical properties of the chiral cyclic TPEs

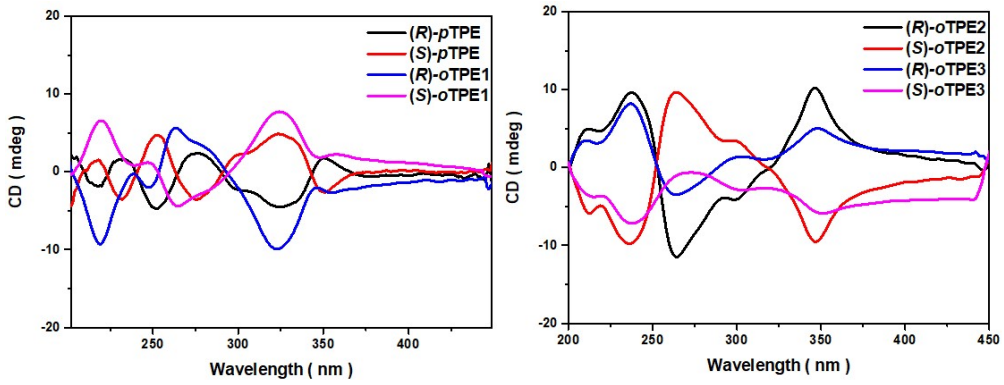

Figure S7. CD spectra of **(*R/S*)-*p*TPE** and **(*R/S*)-*o*TPE1** to **(*R/S*)-*o*TPE3** in 99:1 H_2O/THF.

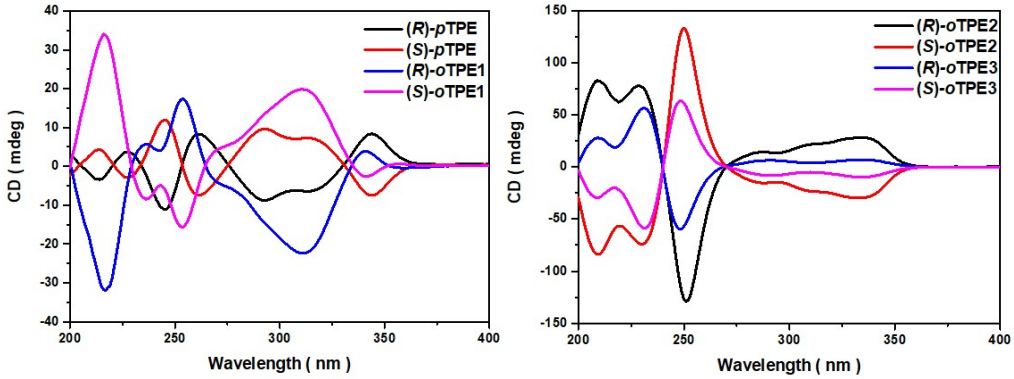

Figure S8. CD spectra of **(*R/S*)-*p*TPE** and **(*R/S*)-*o*TPE1** to **(*R/S*)-*o*TPE3** in the film state.

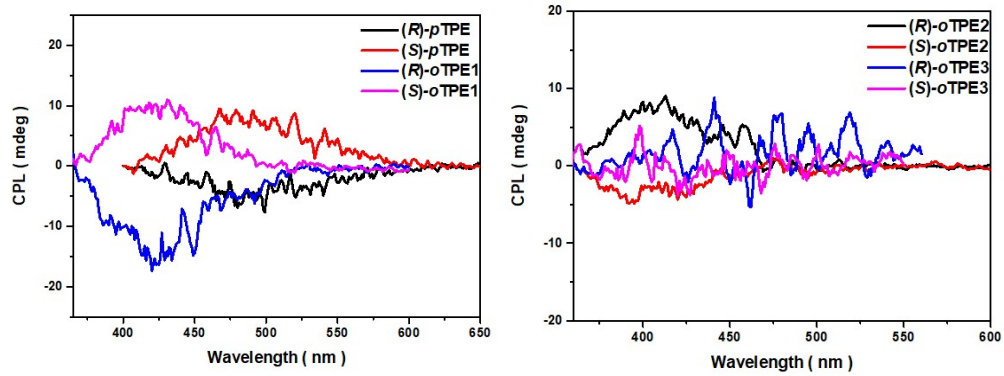

Figure S9. CPL spectra of the **(*R/S*)-*p*TPE** and **(*R/S*)-*o*TPE1** to **(*R/S*)-*o*TPE3** in 99:1 H_2O/THF.

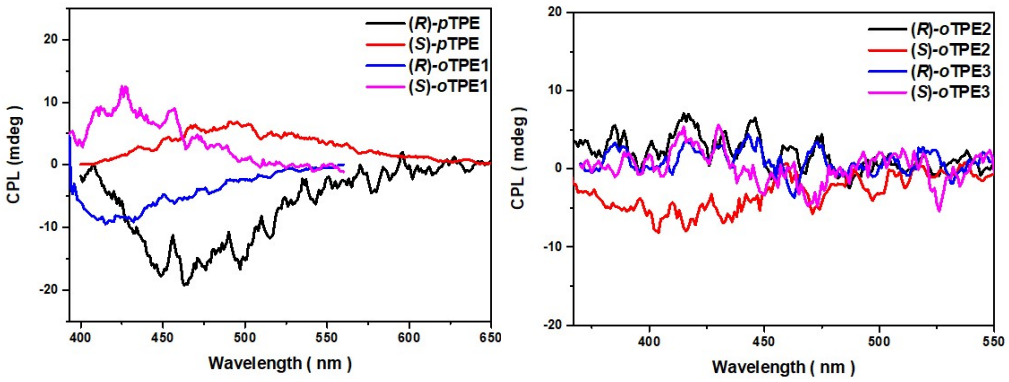

Figure S10. CPL spectra of the **(*R/S*)-*p*TPE** and **(*R/S*)-*o*TPE1** to **(*R/S*)-*o*TPE3** in the film state.

Table S3. Chiroptical properties of the chiral cyclic TPEs in THF solutions.

Compound	λ_{CD} (nm)	g_{abs} (10^{-3})	λ_{CPL} (nm)	g_{lum} (10^{-3})
(*R*)-*pTPE*	312	-1.94	538	-1.97
(*S*)-*p*TPE		1.56		1.97
(*R*)-*o*TPE1	312	-3.78	427	-1.48
(*S*)-*o*TPE1		2.45		1.55
(*R*)-*o*TPE2	312	2.50	411	1.06
(*S*)-*o*TPE2		-3.74		-1.06
(*R*)-*o*TPE3	312	0.50	-	-
(*S*)-*o*TPE3		-1.47		

Table S4. Chiroptical properties of the chiral cyclic TPEs in aggregate and film states.

Compound	99:1 H_2O/THF				Flim			
	λ_{CD} (nm)	g_{abs} (10^{-3})	λ_{CPL} (nm)	g_{lum} (10^{-3})	λ_{CD} (nm)	g_{abs} (10^{-3})	λ_{CPL} (nm)	g_{lum} (10^{-3})
(*R*)-*p*TPE	323	-0.64	498	-1.05	261	1.75	523	-1.33
(*S*)-*p*TPE		0.63		1.20		-1.32		0.88
(*R*)-oTPE1	323	-1.18	425	-1.79	254	1.16	427	-1.75
(*S*)-*o*TPE1		1.12		1.78		-1.30		1.64
(*R*)-*o*TPE2	346	1.37	425	1.25	229	1.37	414	1.38
(*S*)-*o*TPE2		-1.37		-0.91		-1.84		-1.38
(*R*)-*o*TPE3	346	0.46	-	-	231	1.62	-	-
(*S*)-*o*TPE3		-0.41				-1.81		

5. Crystal data and structure refinement for the chiral cyclic TPEs

Table S5. The dihedral angles of the chiral cyclic TPEs.

Compound	A	B	C	D	Binaphthyl
(*R*)-*pTPE*	**56.410(429)°**	48.372(954)°	40.165(790)°	**51.921(771)°**	113.263(376)°
(*R*)-*o*TPE1	**58.831(458)°**	46.335(458)°	**58.256(428)°**	48.483(402)°	83.834(201)°
(*R*)-*o*TPE2	50.945(314)°	52.375(311)°	**56.100(241)°**	**55.443(304)°**	81.306(91)°
(*S*)-oTPE3	**45.609(800)°**	57.548(657)°	42.536(874)°	**65.312(646)°**	98.943(268)°

Table S6. Crystal data and structure refinement for the chiral cyclic TPEs.

Compound	**(*R*)-*p*TPE**	**(*R*)-*o*TPE1**
CCDC	2182870	2182873
Empirical formula	$C_{48}H_{34}O_2$	$C_{48}H_{34}O_2$
Formula weight	642.8	642.8
Temperature/K	150	170
Crystal system	monoclinic	monoclinic
Space group	P 2_1	C 2
a/Å	14.7146(7)	28.682(2)
b/Å	9.8698(5)	11.1603(9)
c/Å	25.4906(12)	27.232(3)
α/°	90	90
β/°	102.8760(10)	112.691(3)
γ/°	90	90
Volume/Å^3	3608.9(3)	8042.2 (12)
Z	2	8
ρ_{calc} g/cm^3	1.261	1.062
μ/mm^{-1}	0.147	0.063
F(000)	1436.0	2704.0
Crystal size/mm^3	0.13×0.06×0.04	0.12 × 0.08 × 0.05
Radiation	MoKα (λ = 0.71073)	MoKα (λ = 0.71073)
2Θ range for data collection/°	3.828 to 50.796	3.960 to 52.798
Index ranges	-17 ≤ h ≤ 17, -11 ≤ k ≤ 11, -30 ≤ l ≤ 30	-35 ≤ h ≤ 35, -13 ≤ k ≤ 13, -29 ≤ l ≤ 34
Reflections collected	38856	34565
Independent reflections	12767 [R_{int} = 0.0970, R_{sigma} = 0.1207	14895 [R_{int} = 0.0646, R_{sigma} = 0.0955]
Data/restraints/parameters	12767/1/928	14895/1/901
Goodness-of-fit on F^2	1.044	1.018
Final R indexes [I>=2σ (I)]	R_1 = 0.0829, wR_2 = 0.2030	R_1 = 0.0704, wR_2 = 0.1628
Final R indexes [all data]	R_1 = 0.1388, wR_2 = 0.2438	R_1 = 0.1227, wR_2 = 0.1987
Largest diff. peak/hole / e Å^{-3}	1.66/-0.59	0.35/-0.26
Flack parameter	0.07(9)	4.9(8)

Compound	***rac-o*TPE2**	**(*S*)-*o*TPE3**
CCDC	2182878	2182879
Empirical formula	$C_{48}H_{48}O_2$	$C_{48}H_{48}O_2$
Formula weight	642.8	642.8
Temperature/K	170	170
Crystal system	triclinic	triclinic
Space group	P -1	P1
a/Å	10.5253(13)	10.2979(5)
b/Å	12.6297(15)	17.4037(10)
c/Å	14.6251(16)	17.5627(9)
α/°	113.373(3)	69.825(2)
β/°	100.425(3)	80.955(2)
γ/°	100.824(4)	81.076(2)
Volume/Å^3	1681.0(3)	2900.4(3)
Z	2	3
ρ_{calc} g/cm^3	1.270	1.104
μ/mm^{-1}	0.076	0.066
F(000)	676.0	1014.0
Crystal size/mm^3	0.08 × 0.05 × 0.03	0.19 × 0.06 × 0.05
Radiation	MoKα (λ = 0.71073)	MoKα (λ = 0.71073)
2Θ range for data collection/°	4.108 to 52.834	4.028 to 52.994
Index ranges	-13≤ h ≤ 13, -15 ≤ k ≤ 15, -16 ≤ l ≤ 18	-12 ≤ h ≤ 12, -21 ≤ k ≤ 21, -22 ≤ l ≤ 20
Reflections collected	18951	33052
Independent reflections	6798 [R_{int} = 0.0959, R_{sigma} = 0.1313]	19422 [R_{int} = 0.0361, R_{sigma} = 0.0602]
Data/restraints/parameters	6798/0/451	19422/2331/1340
Goodness-of-fit on F^2	1.048	1.270
Final R indexes [I>=2σ (I)]	R_1 = 0.0728, wR_2 = 0.1206	R_1 = 0.1096, wR_2 = 0.3006
Final R indexes [all data]	R_1 =0.1803, wR_2 =0.1633	R_1 = 0.1391, wR_2 = 0.3364
Largest diff. peak/hole / e Å^{-3}	0.23/-0.26	1.20/-0.35
Flack parameter	-	-0.8(6)

6. Chiral HPLC analysis of the chiral cyclic TPEs

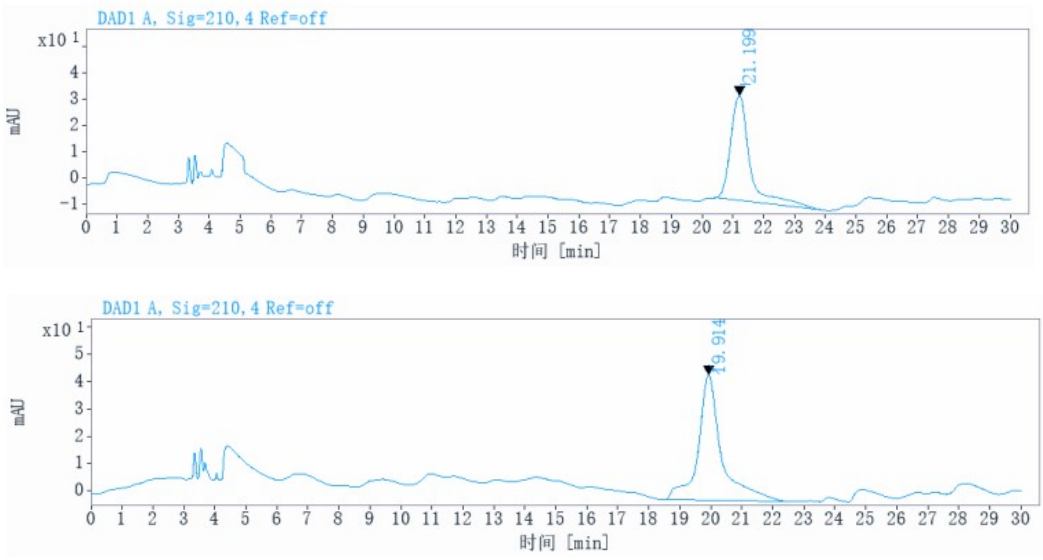

Figure S11. Chiral HPLC spectra of **(*R*)-*p*TPE** (top) and **(*S*)-*p*TPE** (bottom)

Table S7. Chiral HPLC data of **(*R/S*)-*p*TPE**

Sample	Ret. Time (min)	Area (a.u.)	Height (a.u.)	Area (%)	*ee* value (%)	Column	Mobile Phase
(*R*)-*p*TPE	21.199	1754.525	39.944	100.000	100.0	AD	1% *i*-PrOH in hexanes
(*S*)-*p*TPE	19.914	2420.231	45.852	100.000	100.0		

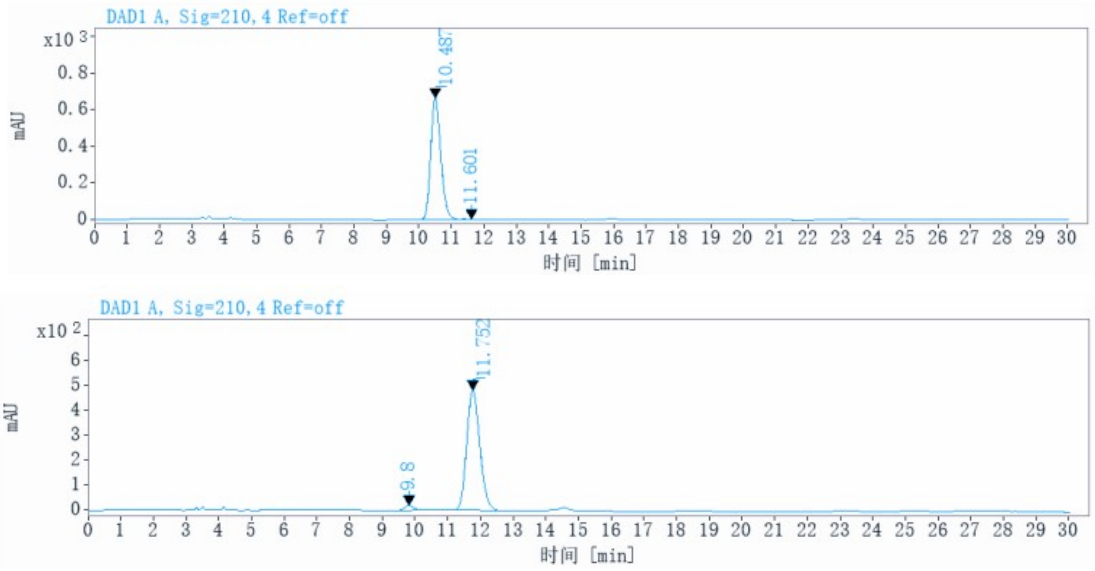

Figure S12. Chiral HPLC spectra of **(*R*)-*o*TPE1** (top) and **(*S*)-*o*TPE1** (bottom)

Table S8. Chiral HPLC data of **(*R/S*)-*o*TPE1**

Sample	Ret. Time (min)	Area (a.u.)	Height (a.u.)	Area (%)	*ee* value (%)	Column	Mobile Phase
(*R*)-*o*TPE1	10.487	14444.527	664.058	99.600	99.2	AD	1% *i*-PrOH in hexanes

	11.601	57.970	1.703	0.400	
(*S*)-*o*TPE1	9.800	440.384	20.920	3.131	93.7
	11.752	13625.050	484.066	96.870	

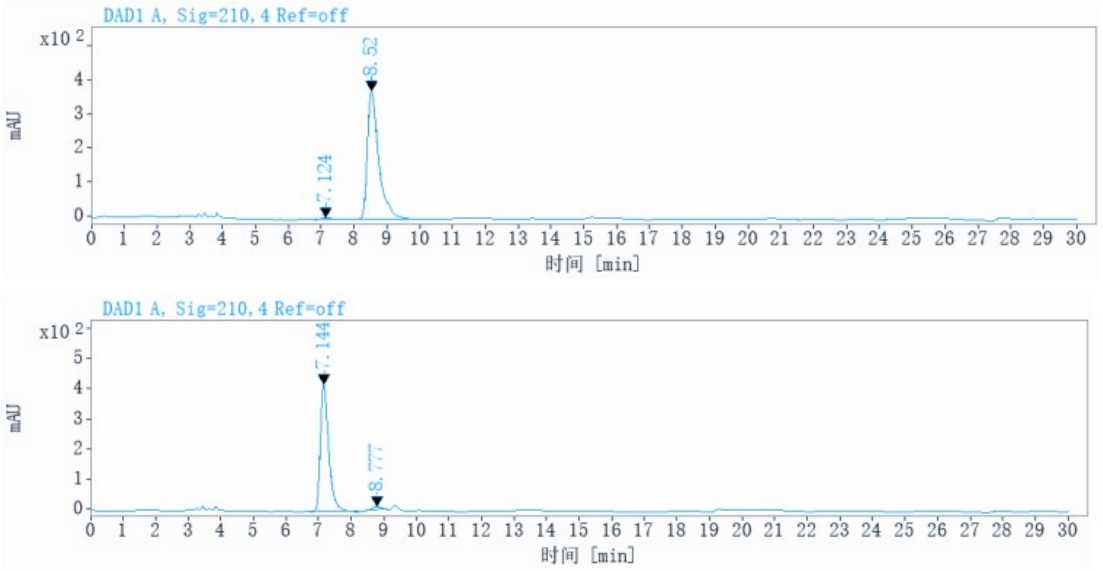

Figure S13. Chiral HPLC spectra of **(*R*)-*o*TPE2** (top) and **(*S*)-*o*TPE2** (bottom)

Table S9. Chiral HPLC data of **(*R/S*)-*o*TPE2**

Sample	Ret. Time (min)	Area (a.u.)	Height (a.u.)	Area (%)	*ee* value (%)	Column	Mobile Phase
(*R*)-*o*TPE2	7.124	115.825	5.494	1.260	97.5	CD	1% *i*-PrOH in hexanes
	8.520	9073.723	374.946	98.740			
(*S*)-*o*TPE2	7.144	7651.361	424.036	96.784	93.6		
	8.777	254.277	12.942	3.216			

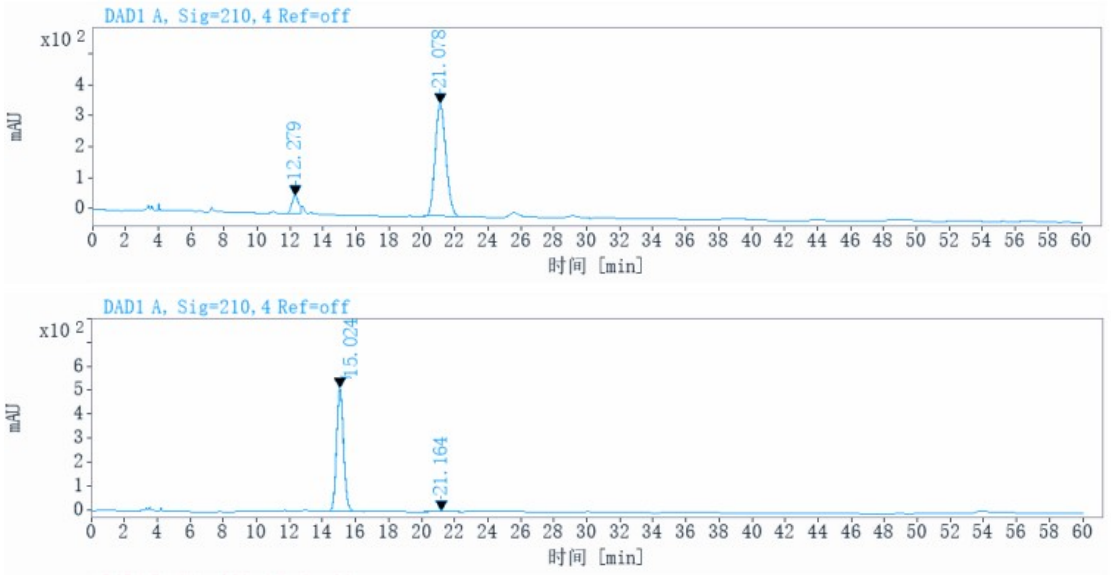

Figure S14. Chiral HPLC spectra of **(*R*)-*o*TPE3** (top) and **(*S*)-*o*TPE3** (bottom)

Table S10. Chiral HPLC data of **(*R/S*)-*o*TPE3**

Sample	Ret.	Area	Height	Area	*ee* value	Column	Mobile Phase

	Time (min)	(a.u.)	(a.u.)	(%)	(%)		
(*R*)-*o*TPE3	12.279	1670.401	58.928	9.061	81.9	AD	1% *i*-PrOH in hexanes
	21.078	16765.477	366.116	90.939			
(*S*)-*o*TPE3	15.024	15380.312	515.613	98.233	96.5		
	21.164	276.591	4.309	1.767			

7. NMR Spectra of the chiral cyclic TPEs

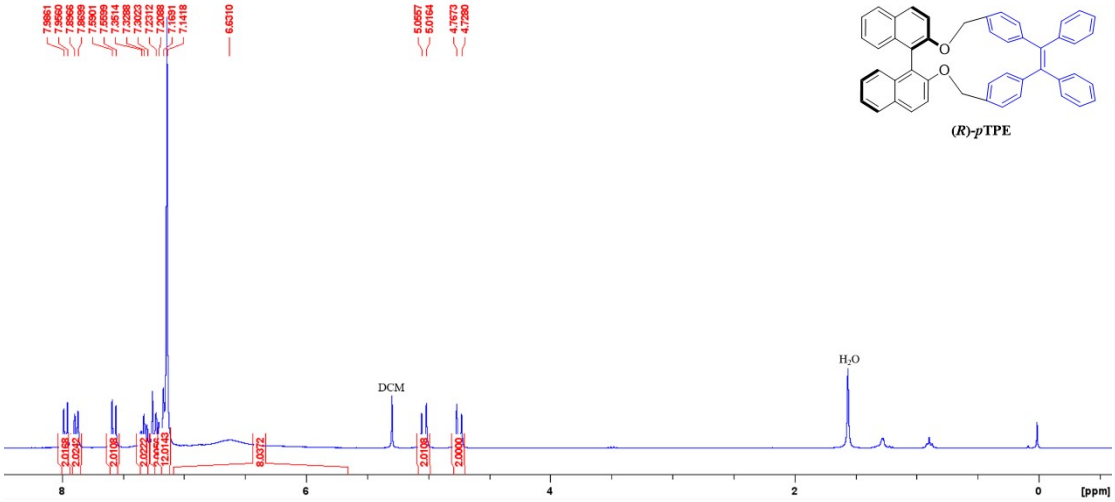

Figure S15. ^{1}H NMR spectrum of **(*R*)-*p*TPE** (300 MHz, $CDCl_3$).

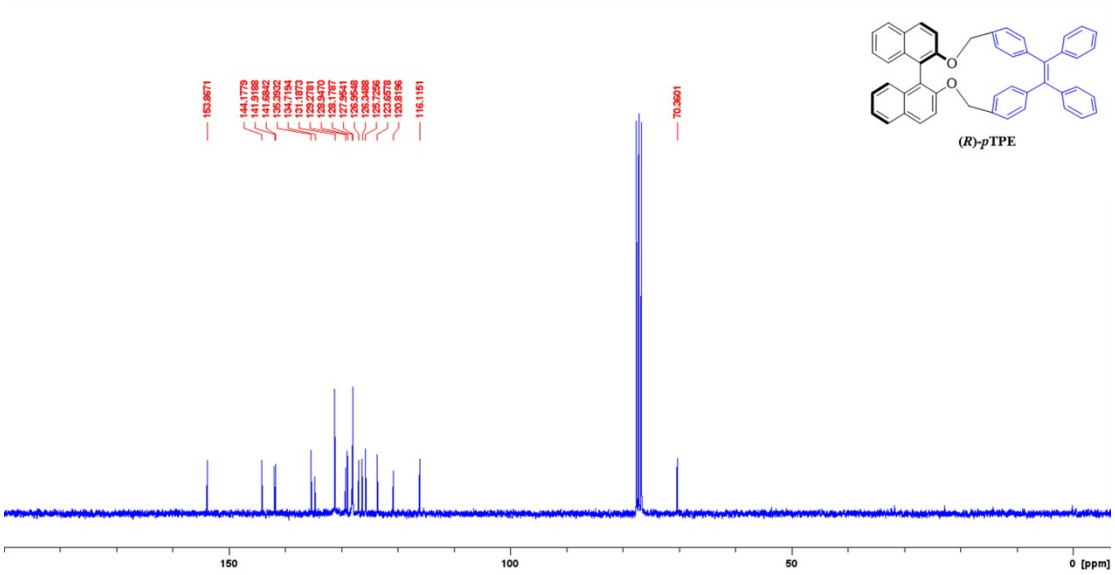

Figure S16. ^{13}C NMR spectrum of **(*R*)-*p*TPE** (75 MHz, $CDCl_3$).

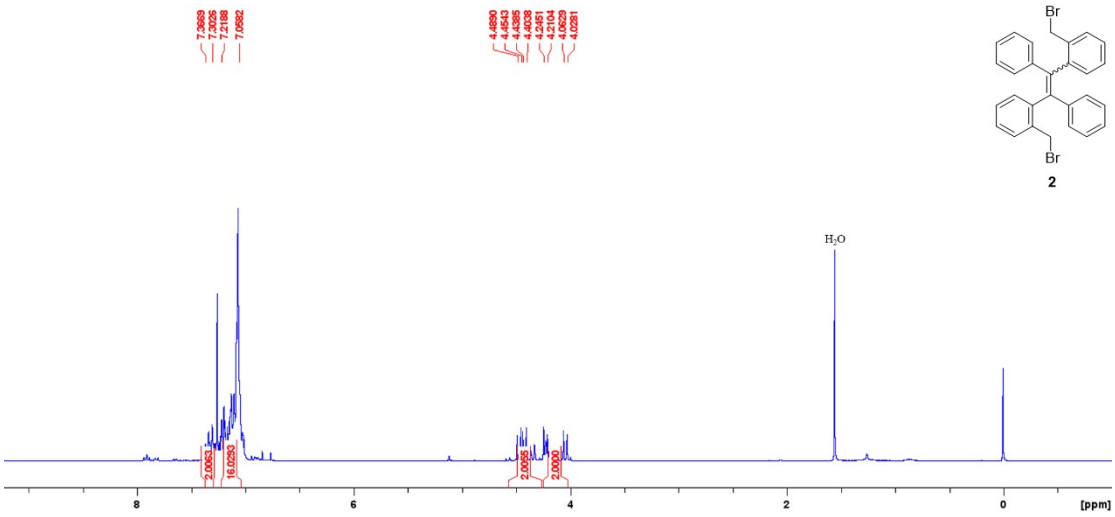

Figure S17. ^{1}H NMR spectrum of **2** (300 MHz, $CDCl_3$).

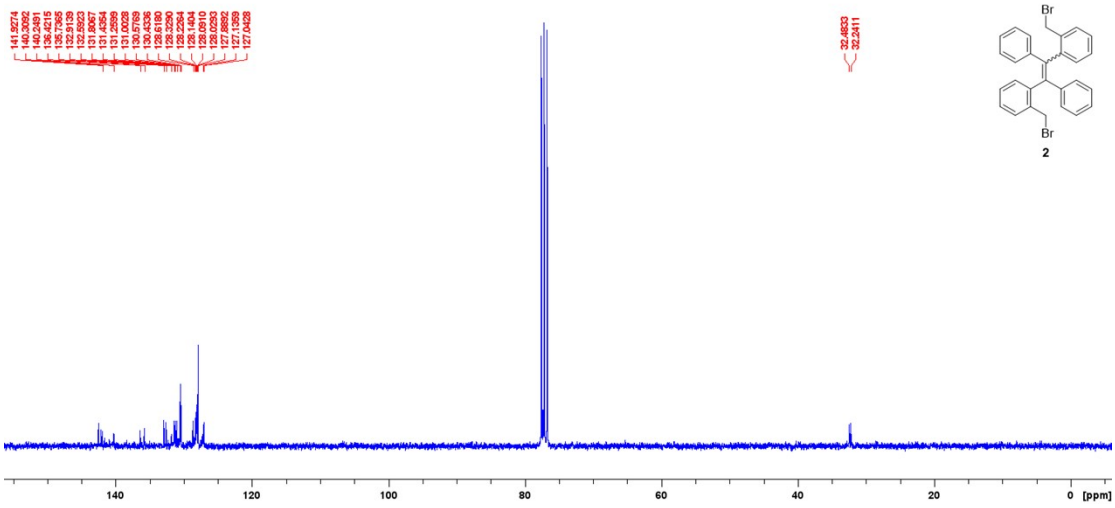

Figure S18. ^{13}C NMR spectrum of **2** (75 MHz, $CDCl_3$).

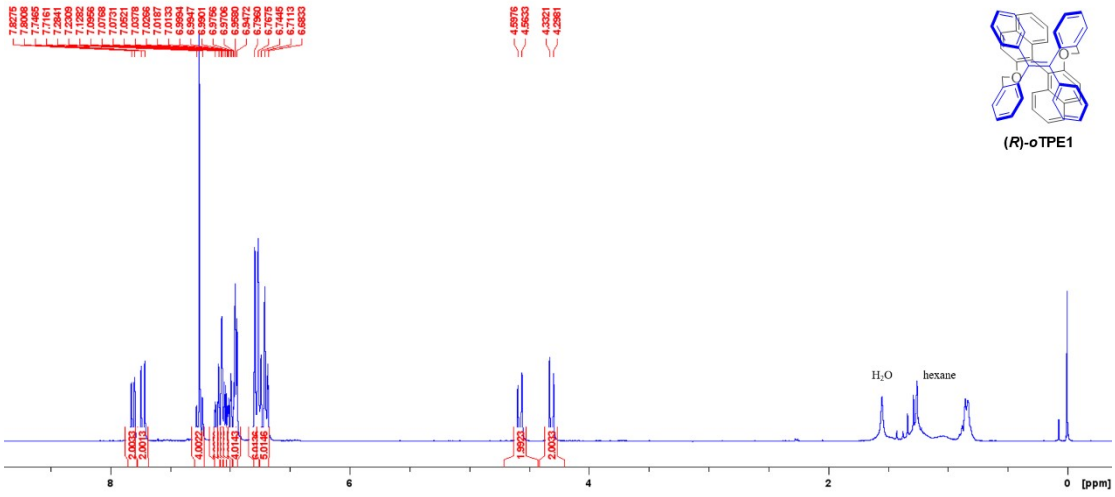

Figure S19. ^{1}H NMR spectrum of **(*R*)-*o*TPE1** (300 MHz, $CDCl_3$).

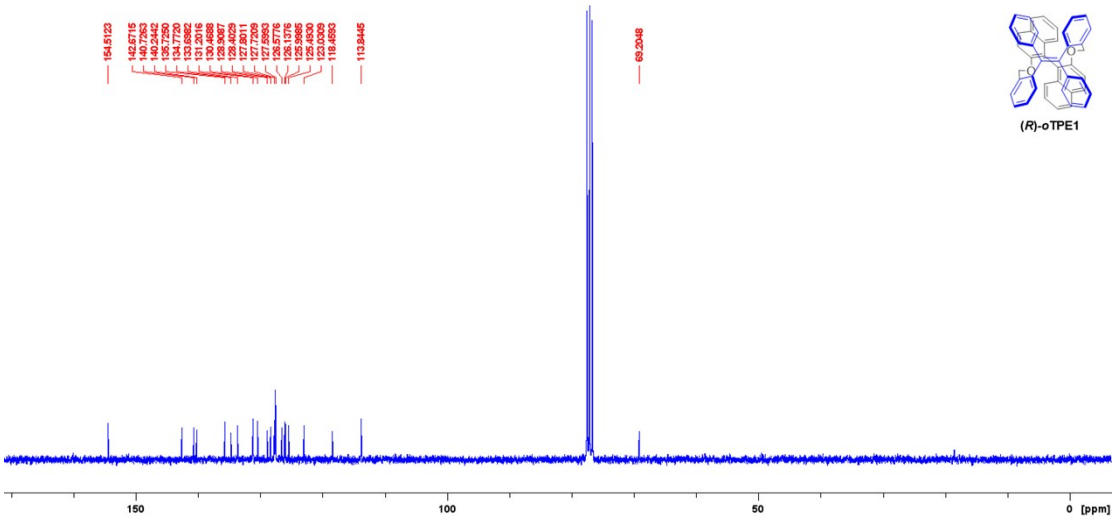

Figure S20. ^{13}C NMR spectrum of **(*R*)-*o*TPE1** (75 MHz, $CDCl_3$).

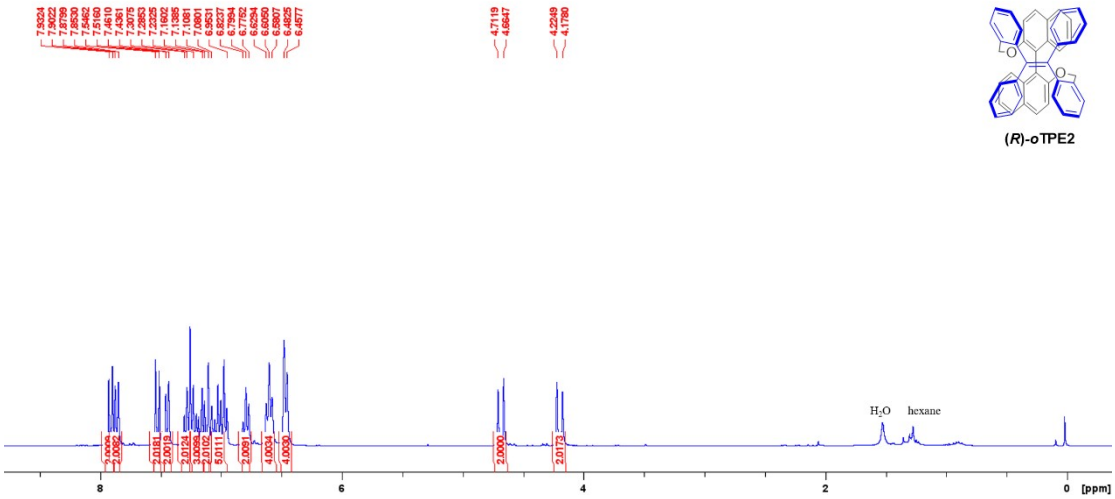

Figure S21. ^{1}H NMR spectrum of **(*R*)-*o*TPE2** (300 MHz, $CDCl_3$).

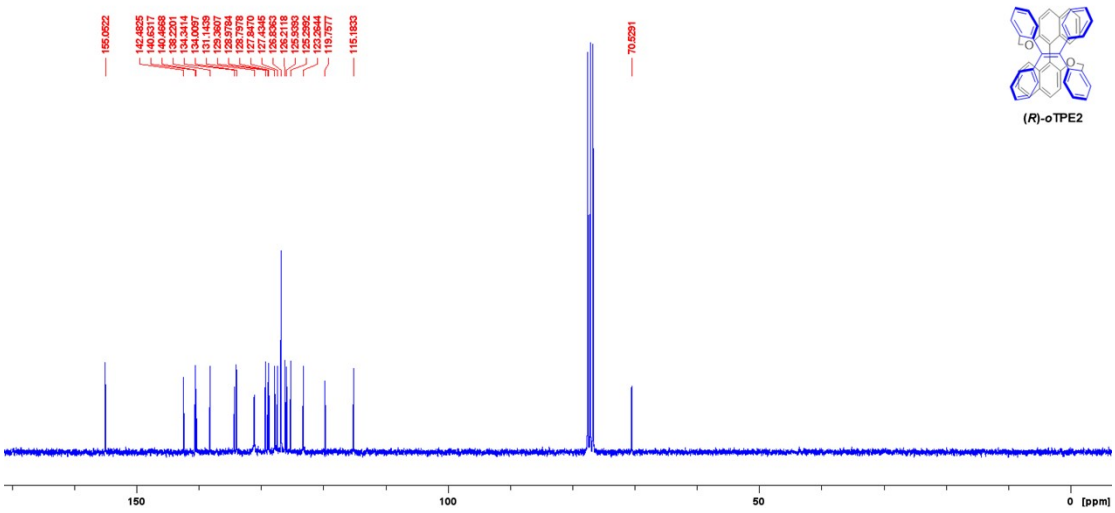

Figure S22. ^{13}C NMR spectrum of **(*R*)-*o*TPE2** (75 MHz, $CDCl_3$).

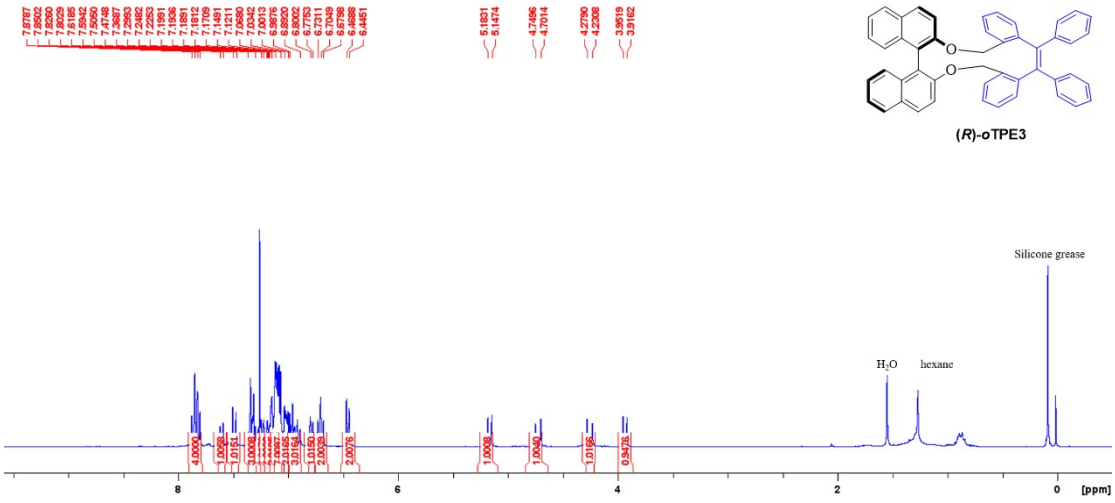

Figure S23. ^{1}H NMR spectrum of **(*R*)-*o*TPE3** (300 MHz, $CDCl_3$).

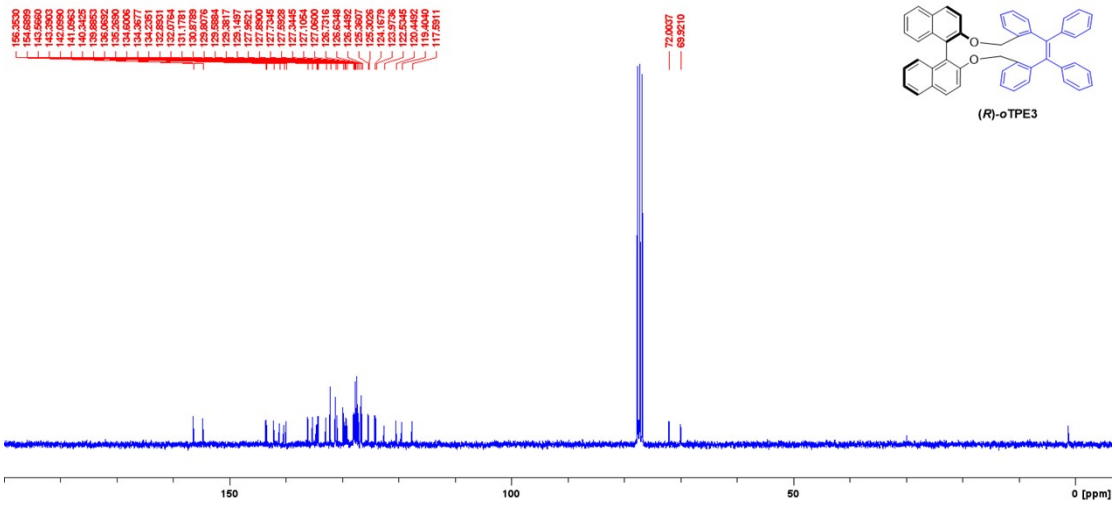

Figure S24. ^{13}C NMR spectrum of **(*R*)-*o*TPE3** (75 MHz, $CDCl_3$).

8. HRMS Spectra of the chiral cyclic TPEs

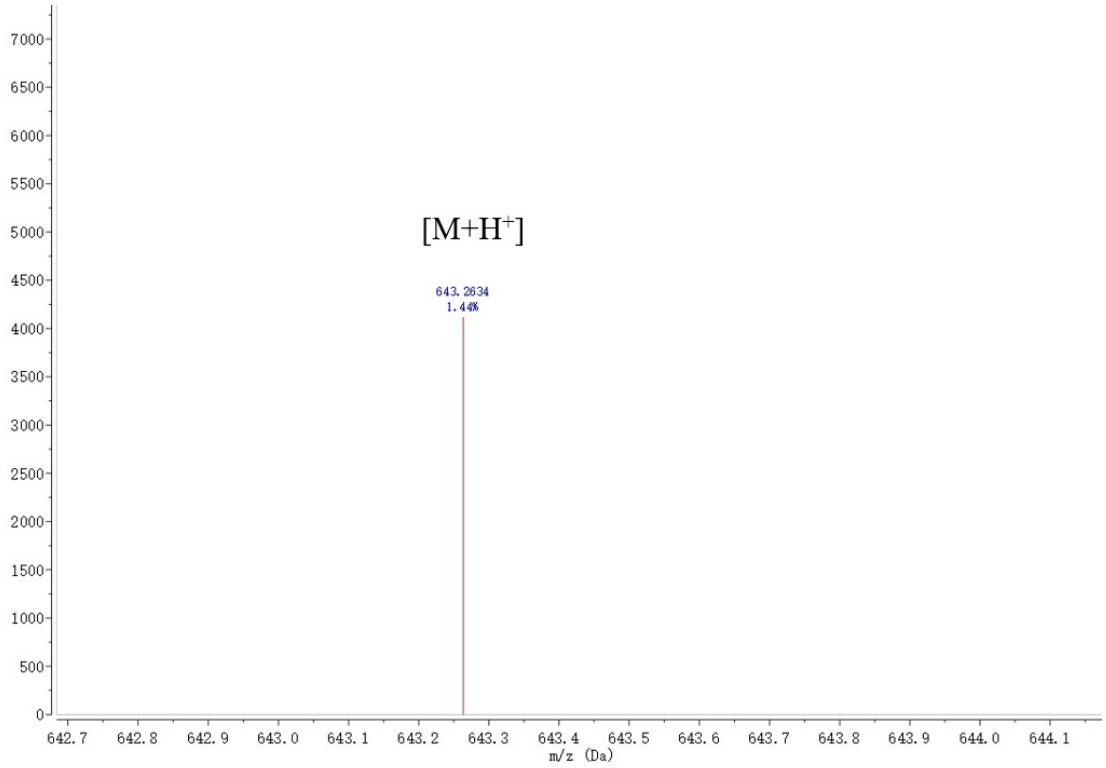

Figure S25. HRMS spectra of **(*R*)-*p*TPE**.

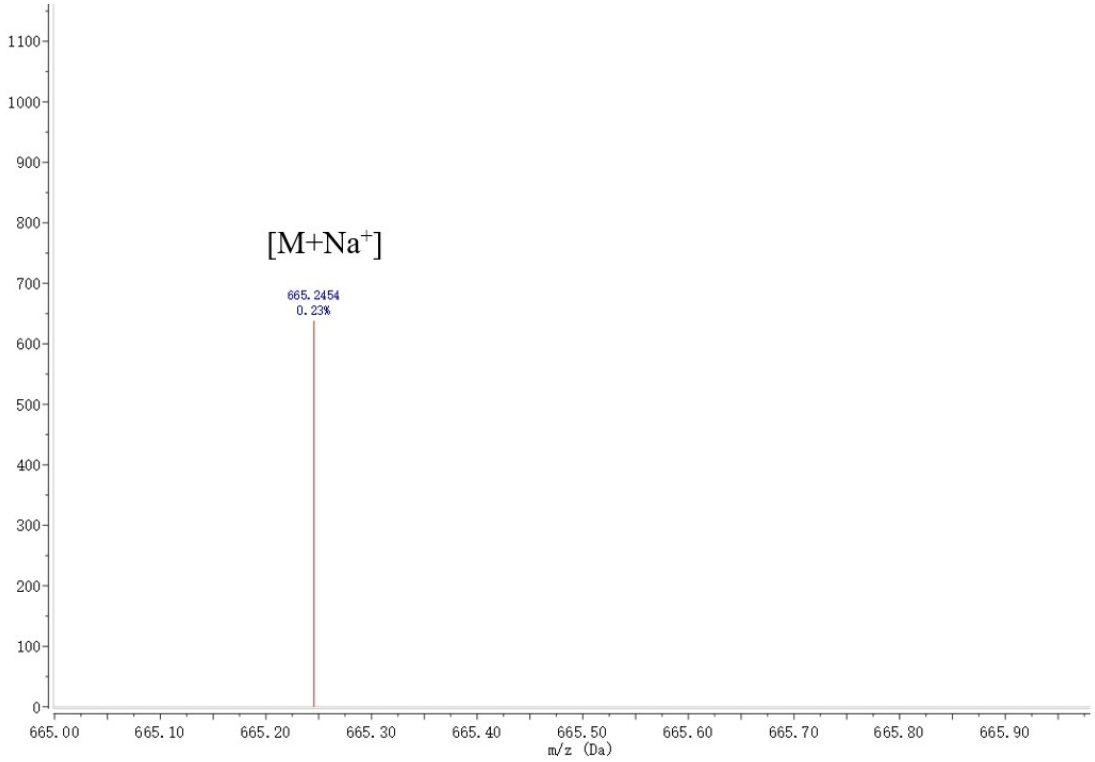

Figure S26. HRMS spectra of **(*R*)-*o*TPE1**.

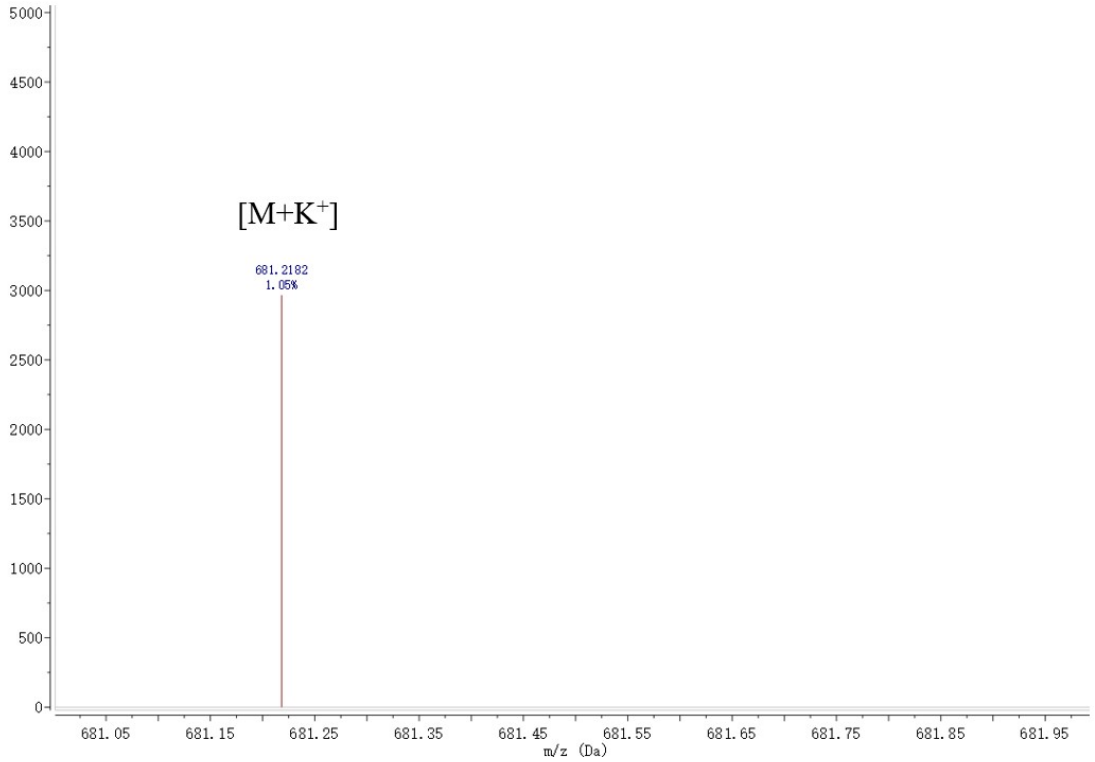

Figure S27. HRMS spectra of **(*R*)-*o*TPE2**.

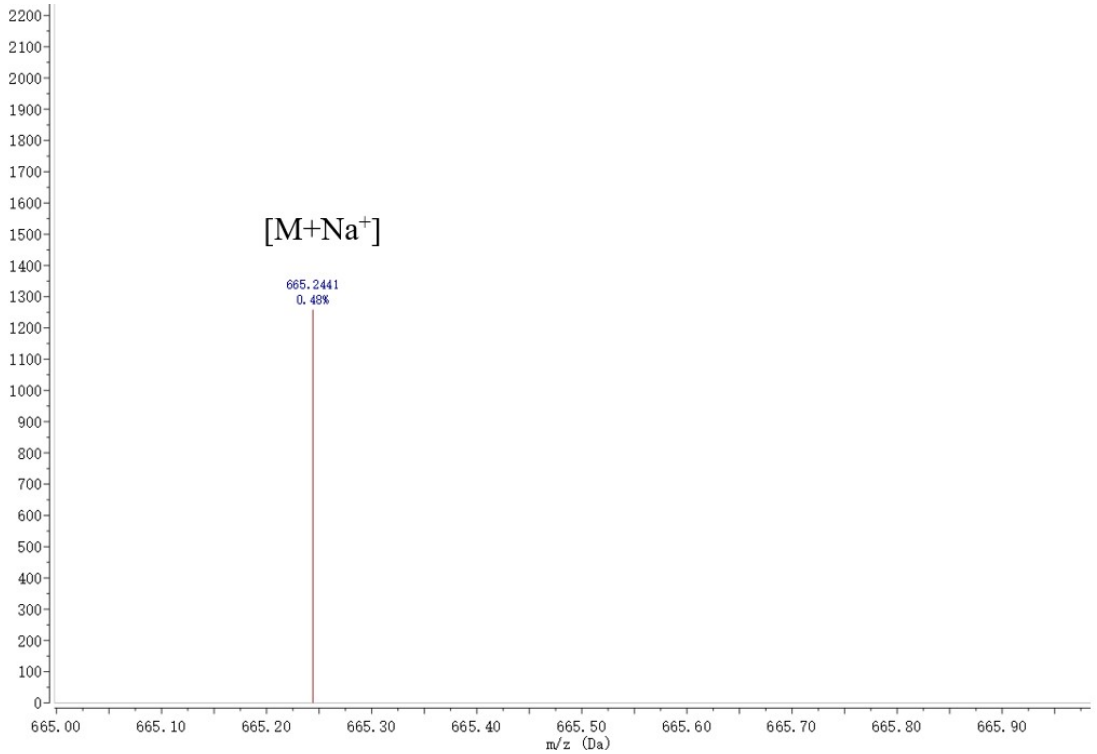

Figure S28. HRMS spectra of **(*R*)-*o*TPE3**.

9. Theoretical calculations of chiral cyclic TPEs

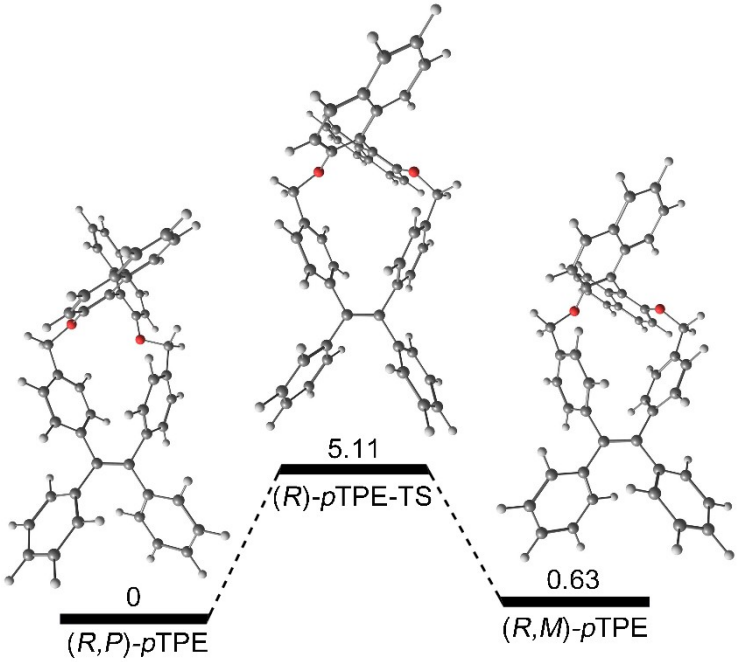

Figure S29. Optimized structures and energy diagrams for the interconversion between (*M*) and (*P*) configurations of **(*R*)-*p*TPE**. The relative free energies are given in kcal mol^{-1}.

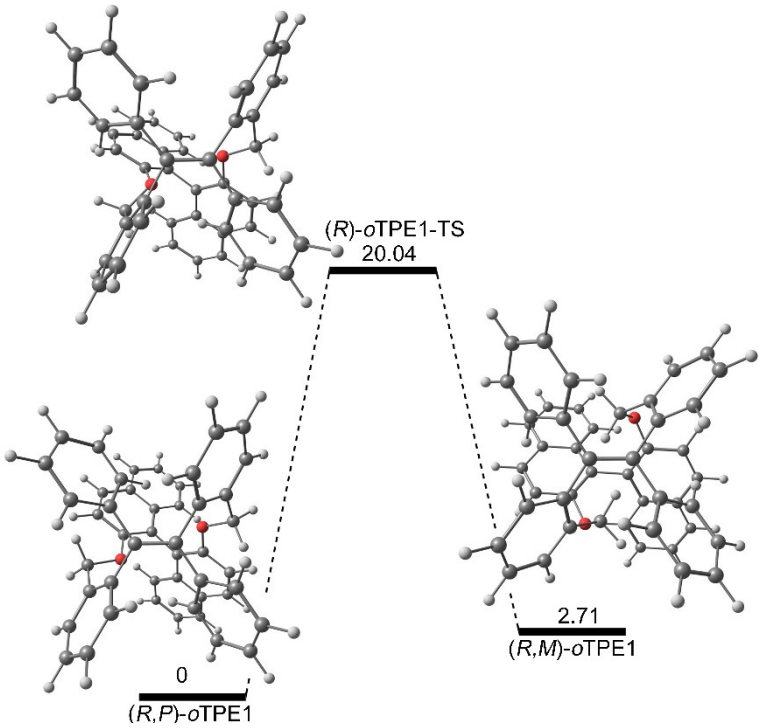

Figure S30. Optimized structures and energy diagrams for the interconversion between (*M*) and (*P*) configurations of **(*R*)-*o*TPE1**. The relative free energies are given in kcal mol^{-1}.

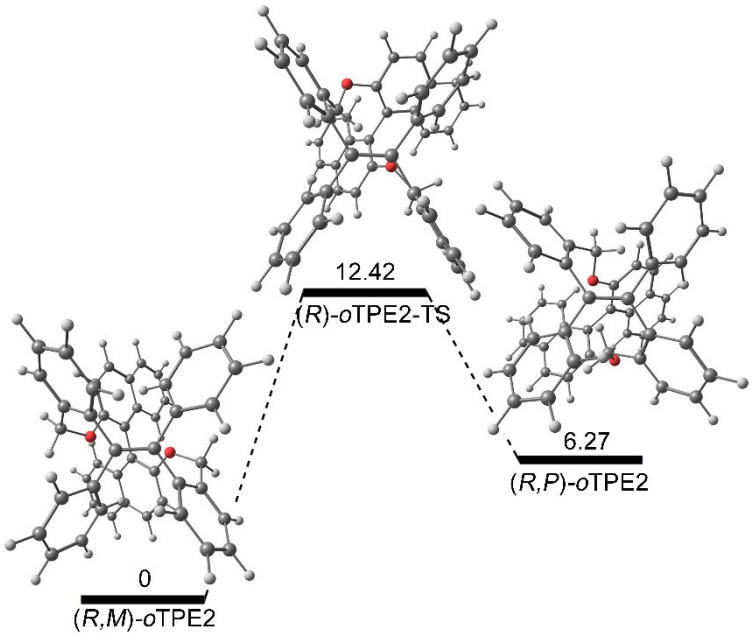

Figure S31. Optimized structures and energy diagrams for the interconversion between (*M*) and (*P*) configurations of **(*R*)-*o*TPE2**. The relative free energies are given in kcal mol^{-1}.

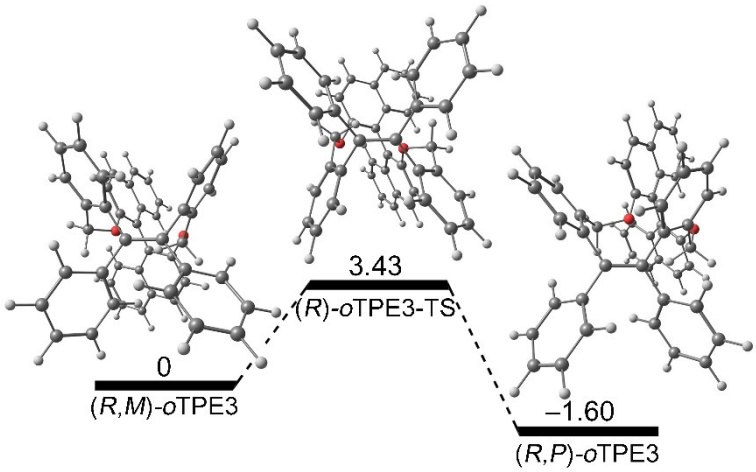

Figure S32. Optimized structures and energy diagrams for the interconversion between (*M*) and (*P*) configurations of **(*R*)-*o*TPE3**. The relative free energies are given in kcal mol^{-1}.